Microstructure of the activated industrial ammonia synthesis catalyst

W. Mahdi, J. Schütze, G. Weinberg, R. Schoonmaker, R. Schlögl * and G. Ertl

Fritz Haber Institut der Max-Planck Gesellschaft, Faradayweg 4, W-1000 Berlin 33, Germany

Received 5 June 1991; accepted 6 August 1991

Industrial doubly-promoted iron catalysts and model systems of singly-promoted K- and Al-iron catalysts were characterised by their catalytic performance at 1 bar pressure. The relevance of bulk nitrogen for catalytic performance is shown. The catalysts were also activated in an in-situ reaction chamber of a He-ion scattering spectrometer (ISS) and their top atomic layer elemental composition was determined after they had reached similar performance as in the microreactor tests. The bulk microstructure of these samples was investigated by high resolution transmission electron microscopy (TEM) and microdiffraction.

All evidence indicates that small highly crystalline α-Fe platelets act as active phase. Their surfaces are covered to a large extent by promotor compounds which are partly present as poorly crystalline aggregates with iron oxide leaving only a small fraction of elemental iron directly exposed to the gas phase. The intimate contact between iron crystals and promoters particles prevents recrystallisation and is the key to the understanding of the structural stability of the catalyst system.

Keywords: Ammonia synthesis; iron catalyst; surface characterization; promoter effects; nitrides; ion scattering spectroscopy; XPS; HRTEM

1. Introduction

Recently [1] the close similarity in temperature programmed desorption (TDS) data for nitrogen from either K-covered Fe(111) single crystal surfaces or an industrial ammonia synthesis catalyst was considered as evidence for bridging the "materials gap" between "real" catalysts and "surface science" model systems, in particular, since the interaction of the catalyst surface with nitrogen represents the rate-limiting step in ammonia synthesis [2]. Very recently [3] conflicting results were reported obtained by a related technique of thermal

* Institut für Anorganische Chemie der Universität Niederurseler Hang, W-6000 Frankfurt 50, Germany

desorption of nitrogen after catalysis at atmospheric pressure. Incomplete activation of the samples used in the first study was suggested to be responsible for the different results.

Little doubt exists in the published literature that the activated technical catalyst contains elemental iron as the active phase [4]. The question of its bulk structure, in particular of its crystallinity was raised, however, several times and attempts were made to link local structural disorder (paracrystallinity) with the catalytic action [5,6]. The observation of non-crystalline iron after activation under non-technical conditions [7] was also used to speculate about the involvement of disordered iron in ammonia synthesis. Intentionally prepared amorphous iron alloys were shown [8], however, to transform into well crystalline iron before high yields of ammonia formation were reached in microreactor tests.

In the present communication a series of results will be presented which were all obtained from technical catalyst samples characterised by their catalytic performance before analysis was carried out. Activation was always done under conditions close to technical prescriptions. In this way it was ensured that materials with a known relation to practical catalysis were analysed. These results are thus considered to close the "materials gap" in a complementary way as it was done in the previous work [1].

2. Experimental

Catalyst samples from the industrial doubly promoted type S-6 (containing, apart from iron, oxides of Si, Ca, Al and K in a total of 5.5 wt%) as well as singly promoted laboratory catalysts promoted either with alumina (2.2 wt%) or with potassium (0.7 wt%) oxide obtained from BASF (Ludwigshafen) were compared to pure iron in the form of commercial Fe sponge (Goodfellows) prepared by hydrogen reduction of Fe oxides. Details of activation and characterisation of these materials are reported elsewhere [5]. BET surface areas of the activated catalysts used in the form of 1 mm sieve fractions of approximately spherical particles were 18 m^2/g (S-6), 22 m^2/g (Al), 4.6 m^2/g (K) and 0.9 m^2/g (sponge).

Conversion tests with $N_2 : H_2$ synthesis gas (1 : 3 molar ratio) at 1 bar pressure and a space velocity of 9600 h^{-1} were done in a stainless steel microreactor (0.600 g catalyst bed) equipped with a non-dispersive infrared ammonia detector. Gas purity was analysed to be below 1 ppm of total water and oxygen.

Surface analysis experiments were carried out using a variable temperature transfer rod which could be moved between a preparation chamber of ca. 2 l total volume used as flow-through reactor for activation and conversion tests (equipped with the same gas supply system and detector as the microreactor) and an analysis chamber equipped with a hemispherical analyser and sources for XPS (Mg K_α), UPS, AES and ISS (He^+, 2 keV, 500 nA sample current, scanning area about 2×4 mm^2). A gas inlet system and a quadrupole mass

analyser allowed in-situ conversion tests at 5×10^{-5} mbar. A 100 μm size sieve fraction of the catalysts was used for these experiments. Transfer times were below 1 min and the residual pressure during surface analysis (mainly hydrogen) was below 3×10^{-9} mbar.

Electron microscopy was done with samples crushed from the 1 mm particles after activation in a glove box and transfered onto usual copper grids under Ar. The grids were also transfered into the microscopes under protection by an Ar stream. Scanning transmission and scanning electron microscopy was done in an analytical JEOL CX 200 instrument with side entry stage at 200 keV electron energy. An attached windowless EDX detector allowed simultaneous elemental analysis of the objects imaged. High resolution electron microscopy at 200 keV and microdiffraction experiments were carried out in a dedicated JEOL CX 200 instrument with top entry stage and image intensifier system.

3. Results

Technical activation procedures were developed with the aim to minimize the peak water gas phase concentration as certain levels damage the activated catalyst [9]. The procedures consist essentially of a slow temperature program extending over ca. 100 hours as were also applied in the present work. After an additional week on stream the degree of reduction at the surface was constant. XPS data presented in fig. 1 clearly indicate a substantial conversion from the initial Fe^{3+} oxide surface to a metallic surface. A detailed analysis of the lineshape shows, however, that part of the iron is only partly reduced which may be accounted for by ternary iron-promoter oxides. These non-reducible oxides are preferentially present at the catalyst surface which offers the explanation for their significant abundance in XPS in comparison to X-ray diffraction and Mössbauer results [5]. Details of the line profile analysis will be reported elsewhere. Here it is important to note that after reduction the surface of the catalyst is indeed reduced to Fe^0 and that there is little probability for possible artifacts in e.g. TDS results caused by inadequate activation.

Conversions reached at 723 K in the surface analysis reactor were ca 60% of the conversion obtained in the microreactor tests which is considered to be reasonable, bearing in mind the non-ideal set-up of a small catalyst bed surrounded by a large gas volume with ill-defined mass transport properties. The level of conversion reached with the different catalysts in the microreactor is shown in fig. 2. The efficiency η is defined as the percentage of the reactor output relative to the equilibrium output at 1 bar total pressure. The limit at ca. 70% η depends on the catalyst bed design and no principal interpretation should be attributed to it.

The beneficial effects of promoters relative to pure iron (XPS surface purity 94% elemental Fe) is very obvious. On a relative scale the addition of "struct-

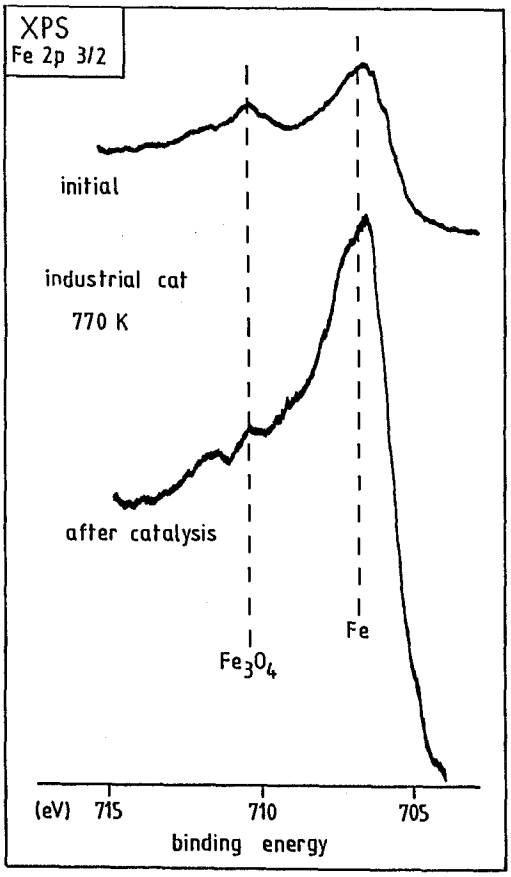

Fig. 1. XPS data of a sample double promoted iron catalyst immediately after reduction and after use in ammonia synthesis at atmospheric pressure.

ural" promoters seems to be more effective than the presence of "electronic" alkali promoters. This is, however, strongly dependent on the pressure of activity testing: at 25 bar and 760 K the conversion by the singly Al promoted catalyst dropped below that of the bipromoted catalyst by ca. 20%. The amount of alumina in the bipromoted catalyst is the same as in the single Al promoted sample which allows to conclude that the addition of K reduces the activity as it reduces the BET surface area.

In the literature the involvement of a surface nitride as well as of nitrogen atoms dissolved in the bulk of Fe in the catalytic cycle was stressed [10]. A non-stationary kinetic test procedure was designed to check the influence of this effect under realistic pressure and gas flow conditions. Fig. 3 presents traces of the ammonia output vs. time at different gas compositions with always identical total flow. Two test temperatures with similar levels of conversion were chosen which are typical for the "thermodynamic" high temperature branch of the conversion vs temperature curve and the "kinetic" low temperature branch.

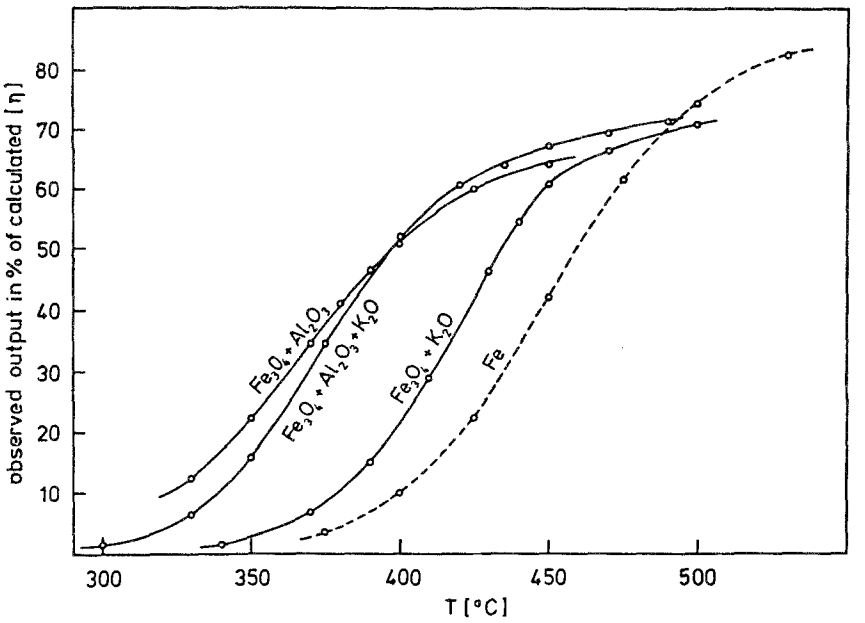

Fig. 2. Conversion expressed as % efficiency relative to equilibrium conversion for differently promoted iron catalysts. The data are corrected for the different BET N_2 surface areas of the materials.

The top level of conversion is given by the steady state under stoichometric gas composition. The conversion decreases rapidly to almost zero level if hydrogen is omitted from the feed indicating that hydrogen is not stored in the

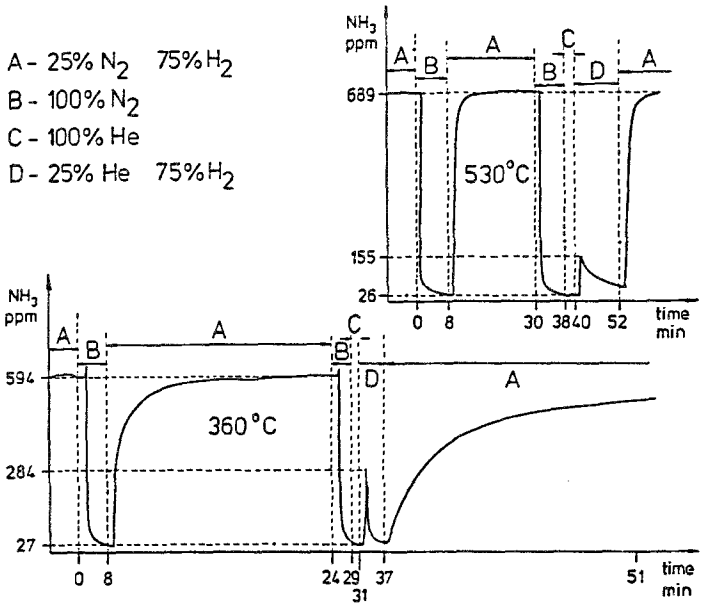

Fig. 3. Conversion vs. time plots for different feed gas compositions.

bulk of the catalyst. The loss of activity is fully reversible with similar time constants at both temperatures. If nitrogen is, however, omitted from the feed and an abrupt admission of hydrogen is achieved, the hydrogenation of nitrogen atoms stored in the bulk of the catalyst can be observed. The evolution characteristics of ammonia are quite different at the two temperatures indicating a rapid surface reaction at the lower temperature which is superimposed by a thermally-activated step effective the high temperature. The ammonia formed at 633 K amounts to ca. 3 μmol which would comprise consumption of only a fraction of a monolayer of atomic β-nitrogen on the 11.7 m^2 catalyst surface in the reactor [11]. The larger amount of ammonia formed at 803 K as well as the slow decay with time indicate that atomic nitrogen is supplied from the bulk storage. This segregation process is too slow at 633 K to be noticeable in the ammonia evolution trace. The involvement of bulk nitrogen in the catalytic cycle is also reflected by the long recovery time for steady state activity needed at low temperature which is absent at the high temperature. The possible alternative explanation by contaminations in the He gas can be rejected after GC and MS analysis of the gas purity.

The elemental composition of the activated catalyst surface was determined by XPS to be 48 at% Fe, 31 at% O, 5 at% K, 2 at% Ca, 8 at% Al and 6 at% carbon impurity. This composition and the strong dominance of the zerovalent iron seen in fig. 1 allow to conclude that the surface consists of islands of iron metal between areas of promoter deposits. A significant amount of contaminating water accounts for the excess of oxygen over the metal ions. This water does not react with the iron metal; a thin layer of material preventing the intimate contact of the water with the iron surface.

The composition of the catalyst surface was studied further by applying the extremely surface-sensitive technique of He ion scattering spectroscopy. The spectra of fig. 4 reflect the elemental composition of the top most atomic layer of the activated catalyst after various treatments. The amount of C and O is strongly underestimated due to the operation conditions of the energy analyser. The surface is dominated by the presence of the promoter elements potassium and calcium. Only about 10% of the exposed surface consists of iron atoms. Due to the many uncertainites with quantitative ISS calibration however, no exact surface compositions were evaluated. The relative abundance of the dominating promoter film did not depend on the conditions of measurement. The inset of fig. 4 illustrates that the signal intensity from the iron atoms, however, is strongly influenced by the pretreatment. Spectrum a corresponds to the activated surface at 300 K (the same for which the XPS was determined). The pronounced apparent discrepancy between ISS and XPS data indicates that the promoter atoms are mainly present as a very thin film transparent for XPS but "shielding" the contamination layer of water from the iron metal.

Heating the catalyst in-situ to 760 K increases the free iron surface. A drastic further increase of free surface iron is observed after admission of hydrogen at

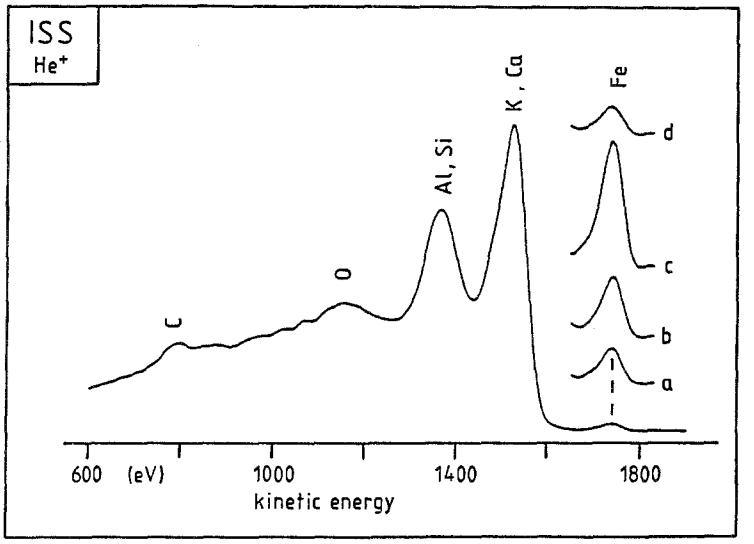

Fig. 4. He ion scattering spectra of double promoted catalyst surfaces. The element assignment is indicated. The iron peak is shown for different treatments after catalysis testing in the same intensity scale: a) at 300 K in UHV; b) at 760 K in UHV; c) at 1×10^{-5} mBar H_2 and 760 K; d) at 1×10^{-5} mBar $H_2 : N_2$ (3 : 1) and 760 K.

1×10^{-6} mbar to the hot surface. The free iron surface is strongly suppressed when a 3 : 1 hydrogen to nitrogen synthesis gas mixture at 1×10^{-5} mbar is applied. This is in line with the expected formation of strongly adsorbed β nitrogen atoms [11], which were, however, not observed directly in ISS due to the very low cross section for nitrogen.

These surface related informations were contrasted with a bulk investigation by electron microscopy. Other bulk techniques such as XRD, Mössbauer spectroscopy and EXAFS agree that the activated catalyst consists to a very large extent of metallic α iron crystals [5]. Scanning electron images of activated catalysts were published earlier [12] in which the existence of a mesopore system was documented.

In fig. 5 the micromorphology is compared between samples of bipromoted catalyst which were either shock-activated or technically activated. Shock activation was done using a linear temperature rise from 300 K to 790 K within 20 min yielding a catalyst with ca. 50% poorer performance than the slowly activated catalyst.

The low resolution images show segregated promoter oxide species. Slow activation gave rise to the growth of well-crystalline platelets of Ca-Fe-oxide, shock heating produced whisker-like structures of inhomogeneous Al-Si-K-Ca-Fe oxide. In both images the formations of iron grains with ca. 100 nm size and the evolution of a pore structure can be seen. The BET surface area were 18.4 m^2g^{-1} for the slowly activated catalyst and 15.0 m^2g^{-1} for the shock heated sample.

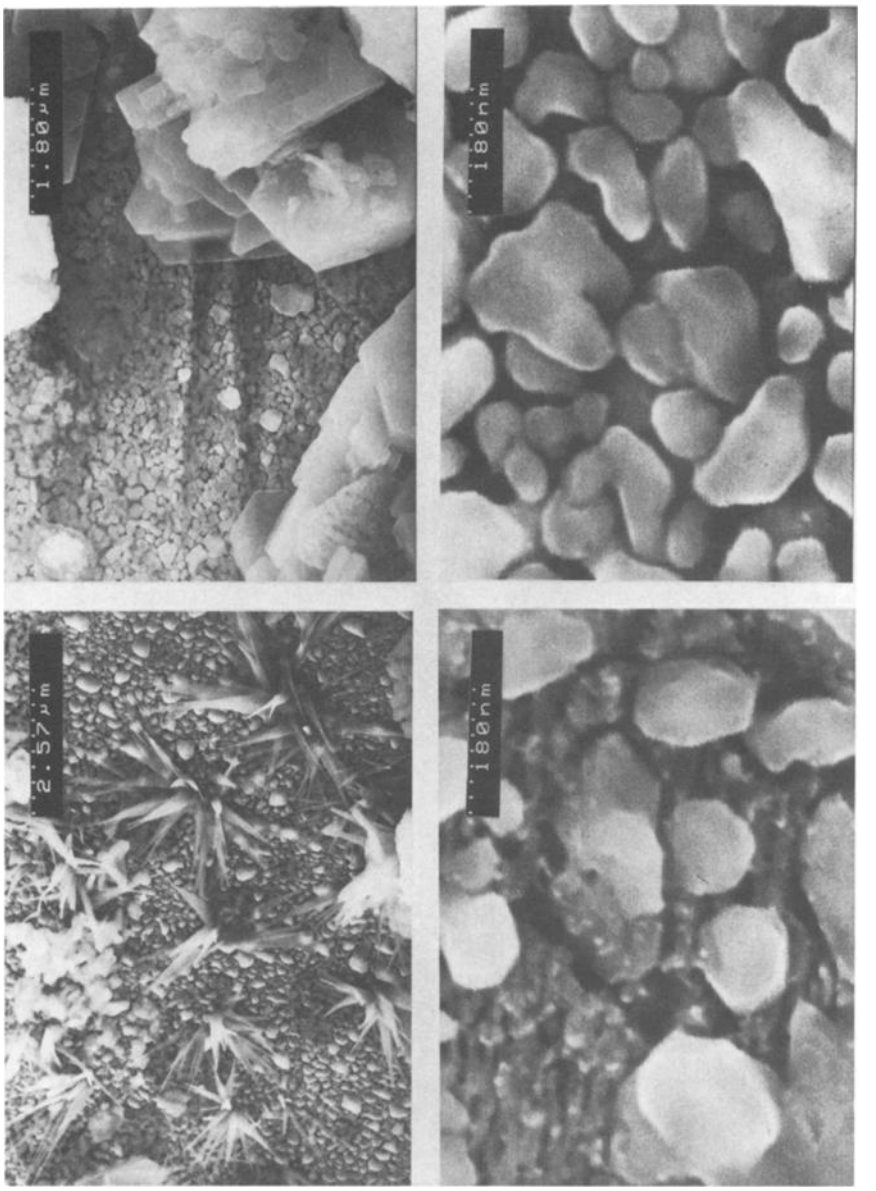

Fig. 5. SEM micrographs at two different resolutions for slowly activated (right) and shock-activated (left) double promoted industrial catalysts.

The two high-resolution images reveal that in both cases iron crystals of similar shape and size have formed. These crystals are the only species in the slowly activated sample. The shock heated material contains a second large

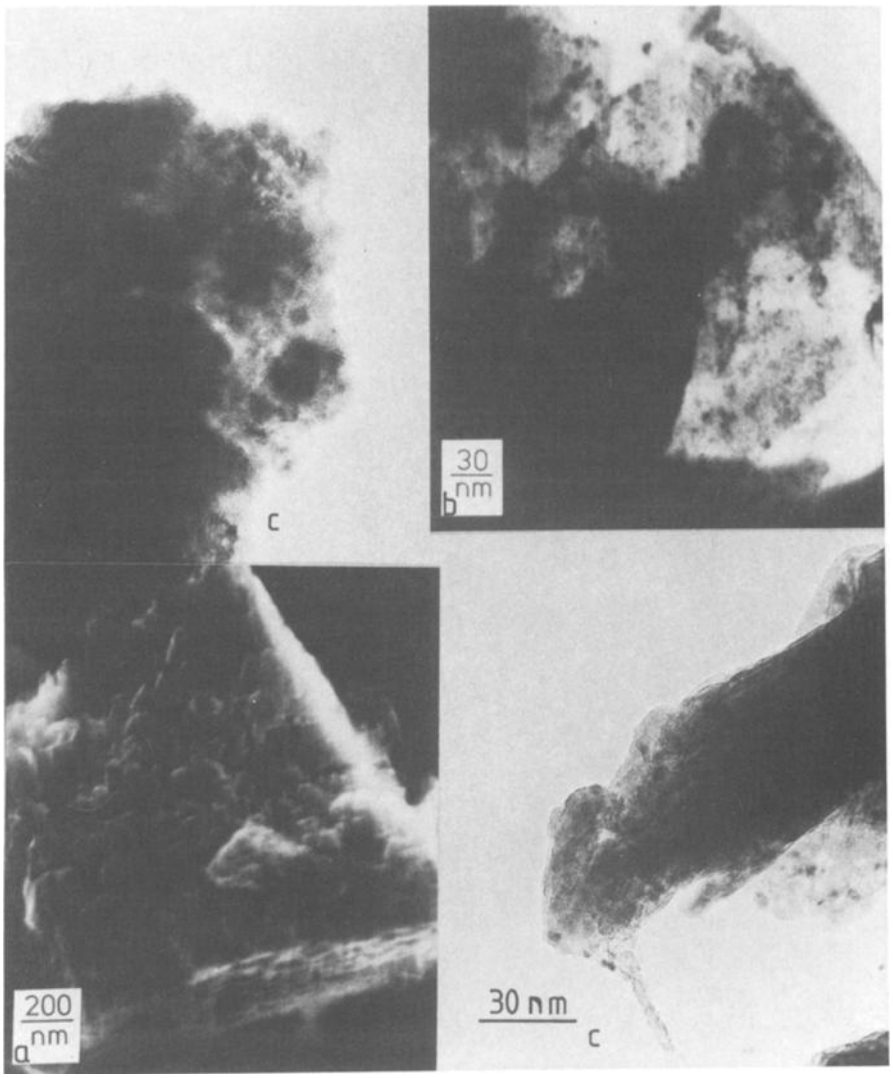

Fig. 6. Microstructure of the "compact" Fe-crystals" seen in fig. 5 bottom with higher resolution: a) in SEM; b) in STEM; c) in TEM. All images were taken with 200 keV acceleration voltage.

fraction of material which may consist of stacks of platelets with the prism faces of the stacks viewed in the image. The little dots arise from Ca-K-Fe-oxides.

Both morphologies can not be observed in the catalyst precursors which underlines the effect of restructuring [13] occuring during the solid state chemical processes of "reduction" of the precursor oxide mix.

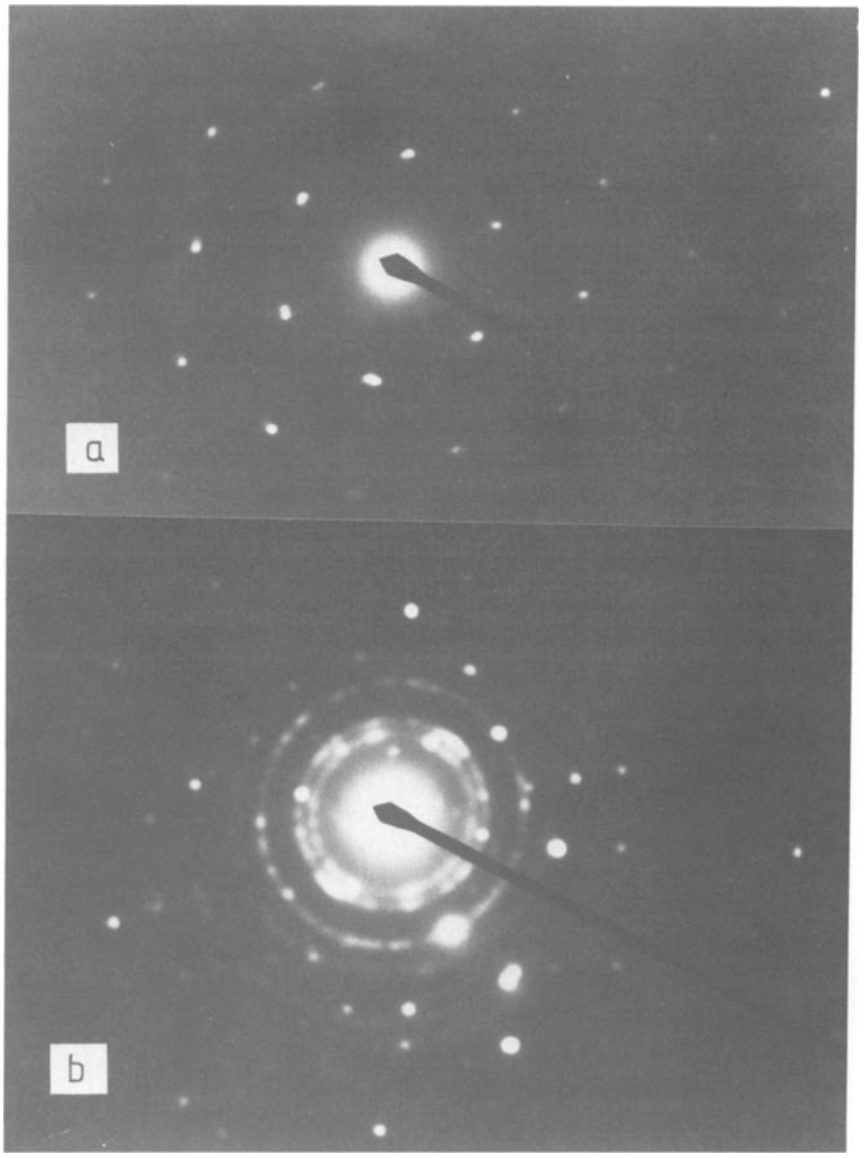

Fig. 7. Microdiffraction patterns of individual Fe metal platelets and aggregates of Fe-promoter oxides.

With higher resolution, the regular shaped "compact" iron crystals are neither compact nor homogeneous as can be seen from fig. 6 presenting a summary from SEM (a), STEM (b) and TEM (c) observations. These images show that the large crystals are made up from stacks of platelets held apart from each other by spacers of particulates which consist of iron-promoter oxides not reducible at the catalyst operation temperatures. These dots of "impurities" prevent the sintering process of the iron platelets into large isotropic crystals. The presence of all promoter elements plus some oxygen at this level of resolution was shown by EDX and is discussed in detail elesewhere [5].

The primary platelets may occur in the catalyst either in a neatly stacked version as compact "crystals" after slow activation or in a more disordered form with large voids in between caused by segregated large promotor oxides in the shock-heated samples. It is thus the activation process which decides via the aggregation kinetics of the promoter oxides which stacking order of the platelets will occur.

The activation also controls the degree of internal reduction of the platelets. Electron microdiffraction reveals two characteristic patterns shown in fig. 7. In the slowly activated catalyst the pattern of crystalline iron (a) can be found

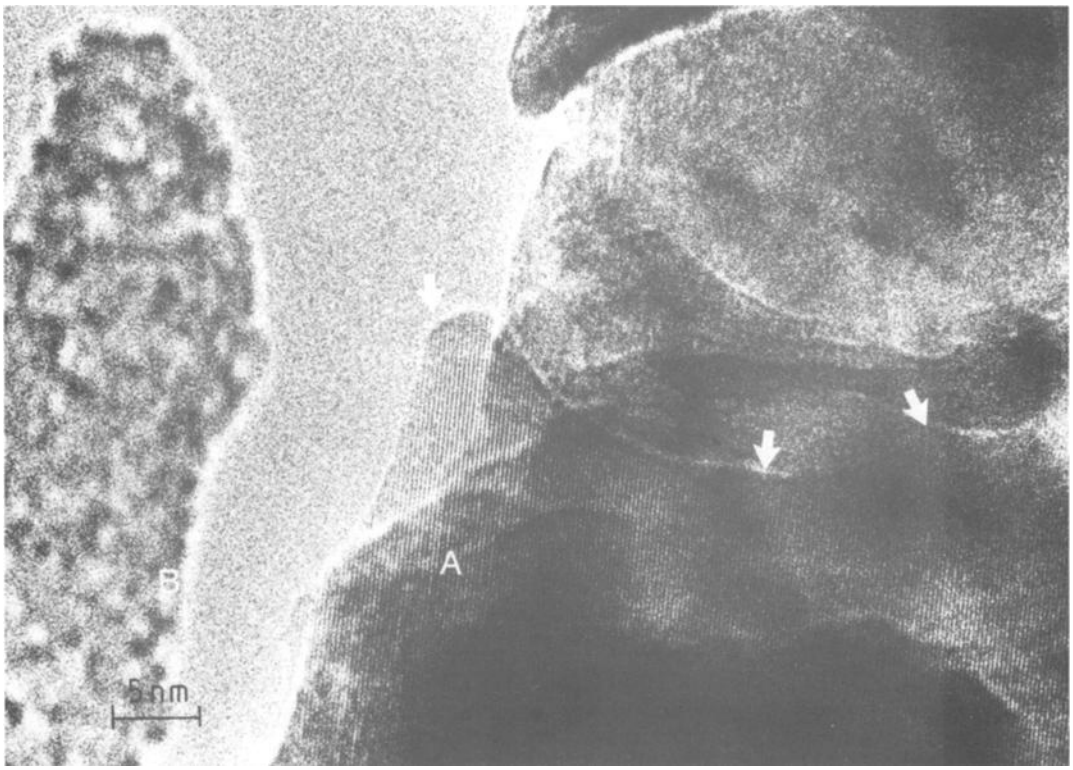

Fig. 8. High resolution TEM image of a single Fe metal platelet.

frequently. This pattern is formed if the electron beam is normal to the platelet surface and thus indicates the basal plane of the platelets to be the (111) face.

Much more dominating was diffraction pattern (b) in the shock heated catalyst. It arises from microcrystalline Fe_3O_4 with even amorphous oxide contributions (rings). The weak spots following the intense double ring occur from elemental iron and vary considerably in intensity from particle to particle.

Both patterns of well- crystalline iron metal and microcrystalline spinel oxide can be found in both activated catalysts with quite different frequency [14]. It is concluded that both structures are thus relevant for the operation of the catalyst with the correctly activated sample containing a minimum of the oxide material and a maximum of well-ordered iron metal.

This well-ordered iron metal can be seen in fig. 8 presenting (111) lattice fringes of α iron resolved in one individual platelet (region "A") of the slowly activated catalyst. The stack structure of the secondary "crystal" becomes also quite apparent. Amorphous material such as the carbon particle support gives rise to the contrast of region "B".

4. Conclusions

Experimental evidence based on kinetic, spectroscopic and morphological data allow to conclude that the action of the technical ammonia synthesis catalyst is indeed correlated with the presence of well-ordered α-iron in (111) orientation, i.e. that model studies of promoted Fe (111) single crystals are very close to reality. The presence of "structural" promoter elements during activation and later during application is essential for the organisation of the α-iron in such a metastable arrangement susceptible to sintering into isotropic pure α-iron and segregated promoter oxides.

This sintering does not occur during correct activation but may damage an activated catalyst at any later time if a thermal shock treatment is applied. This may occur for instance by admission of oxygen to the operating catalyst causing a rapid overheating. If a thermal shock is applied for activation, the resulting catalyst is distorted in the arrangement of the primary iron platelets and in the proportion of iron metal to iron oxide present resulting in a poorer catalytic performance. Such an activation was used in the in-situ X-ray diffraction study claiming the nature of the activated catalyst being poorly crystalline [7]. The fact that pure unpromoted iron oxide used in this study as reference material did not exhibit this kinetic sensitivity for the formation of iron metal indicates that it is the presence of the promoter elements during activation which causes the special properties of the catalytic iron in ammonia synthesis.

Acknowledgements

We thank A. Reller (Zürich) for collaboration with the TEM work. High resolution SEM images were obtained at the instrument of D.D. Jefferson (Cambridge, UK). Financial support from Fonds der Chemischen Industrie und Hermann Willkomm Foundation is gratefully acknowledged. Catalyst samples were kindly provided by ICI (UK), BASF (FRG) and Haldor-Topsoe (DK).

References

[1] R. Schlögl, R.C. Schoonmaker, M. Muhler and G. Ertl, Catal. Lett. 1 (1988) 237.
[2] P. Stoltze, Physica Scripta 36 (1987) 824.
[3] H.D. Vandervell and K.C. Waugh, Chem. Phys. Lett. 171 (1990) 426.
[4] G. Ertl, J. Vac. Sci. A1 (1983) 1247.
[5] R. Schlögl, in: *Science and Technology of Ammonia Synthesis*, ed. J.R. Jennings (Plenum, 1991) in press.
[6] D.C. Silverman and M. Boudart, J. Catal. 77 (1982) 208.
[7] T. Rayment, R. Schlögl, J.M. Thomas and G. Ertl, Nature 315 (1985) 311.
[8] A. Baiker, R. Schlögl, F. Armbruster and H.J. Güntherodt, J. Catal. 107 (1987) 221.
[9] A. Baranski, A. Reizer, A. Kotarba and E. Pyrczak, Appl. Catal. 19 (1985) 417.
[10] G. Ertl, M. Huber and M. Thiele, Z. Naturforsch. 34a (1979) 30.
[11] M. Grunze, M. Golze, J. Fuhler, M. Neumann and E. Schwartz, *Proc. 8th ICC*, Vol. 4 (1985) 133.
[12] G. Ertl, D. Prigge, R. Schlögl and M. Weiss, J. Catal. 79 (1983) 359.
[13] D.R. Strongin, S.R. Bare and G.A. Somorjai, J. Catal. 103 (1987) 289.
[14] A. Nielsen, *An Investigation on Promoted Iron Catalysts for the Synthesis of Ammonia*, 3rd ed. (Gjellerup, 1968).